COMMUNICATION

Check for updates

Deoxygenation of heterocyclic *N*-oxides employing iodide and formic acid as a sustainable reductant†

Alicia Elvira Cruz-Jiménez,‡[a] Paola Alejandra Argumedo-Castrejón,‡[a]
Jeferson B. Mateus-Ruiz,‡[a] Victor A. Lucas-Rosales, [iD] ‡[b] Octavio Adrián Valle-González, [iD] [a] J. Oscar C. Jiménez-Halla[b] and J. Armando Luján-Montelongo [iD] *[a]

We present a novel deoxygenation method for heterocyclic *N*-oxides utilizing iodide as a catalyst. Iodide acts as a reducing catalyst that is regenerated by formic acid, which also serves as a Brønsted activator and solvent. The method demonstrates high efficiency and excellent selectivity in the reduction of a variety of heterocyclic *N*-oxides and tertiary amines. Our computational DFT investigation revealed that the reduction mechanism entails a direct interaction between iodide and the oxygen of the *N*-oxide within a Mg^{2+}/formic acid framework, resulting in the formation of the *N*-heterocycle and the release of a hypoiodite unit. Additionally, a molecular mechanism for the regeneration of iodide from hypoiodite, facilitated by formic acid, is suggested. This method provides an environmentally friendly approach for the deoxygenation of *N*-oxides and related species.

Pyridines and quinolines are fundamental heterocyclic structures, extensively found in natural products,[1] and playing pivotal roles across various fields. Their significance ranges from their inherent presence in biologically active compounds[2] to applications in medicinal chemistry (Fig. 1a),[3] and materials science.[4] In consequence, compounds containing *N*-pyridinic moieties are among the most commonly used in the manufacture of drug candidates.[5] Unfortunately, the direct functionalization of pyridines and their derivatives through direct electrophilic substitutions imposes a challenge due to poor chemoselectivity and a lower π-system energy compared to benzene.[6] A compelling strategy for effective pyridine functionalization involves the use of *N*-activated pyridines,[7] among which *N*-oxide derivatives (Fig. 1b), with remarkable availability and reactivity, enable functionalization

through various strategies.[8] Therefore, after the functionalization of pyridine/quinoline *N*-oxides, regeneration of the *N*-heterocycle through deoxygenation would be needed. Among the reductant systems used for heterocyclic *N*-oxide deoxygenation (NOD) many are based on transition metals (TM)[9] including Mo, Pd, In, Ir, Ru, Sm, *etc.*, while other TM-free based methods are found in lesser extent.[10]

Iodine-based deoxygenations of *N*-functionalities have emerged as alternatives,[11,12] particularly since some methods employ green sacrificial reductants.[12] In the case of iodide-based methodologies for NODs, iodide is often used as a sacrificial reductant, in stoichiometric or superstoichiometric quantities, and often paired with metals, including TMs.[13]

The search for cost-effective, efficient, and environmentally friendly methods for the selective reduction of heterocyclic *N*-oxides is crucial. Formic acid (FA) has emerged as a prominent reducing agent.[14] Furthermore, its production from biomass or CO_2 valorization adds a sustainable appeal.[15] Recently, we introduced the I^-/FA as a green reagent for reducing methylsulfinates and sulfoxides (Fig. 1c).[16] This method utilizes iodide as the catalytic reductant, which is regenerated by formic acid. Additionally, formic acid serves both as the medium/solvent and in the elaboration of an activating Brønsted template. Under the optimal conditions, we observed exceptional reducing efficiency, coupled with remarkable orthogonality to various reducible functional groups.

Following our research program, which focuses on the development of TM-free[16,17] and iodine/iodide-based synthetic methods,[16,18] we present a practical method that enables the deoxygenation of pyridine *N*-oxides (and related species such as *N*-oxides derived from quinolines, isoquinolines and tertiary amines) using the I^-/FA reagent. Our experimentation began exposing quinoline *N*-oxide (**1a**) to KI (10% mol) in formic medium, under MW irradiation, delivering 40% yield of quinoline (**2a**) (entry 1, Table 1). As expected, iodide was essential for the reduction as the absence of KI or its replacement by potassium salts such as K_2SO_4 and K_2HPO_4 delivered no reduced product (entries 2–4). Other iodide sources such as

[a] *Departamento de Química, Centro de Investigación y de Estudios Avanzados (Cinvestav) Av. Instituto Politécnico Nacional 2508 San Pedro Zacatenco, 07360 Ciudad de México, Mexico. E-mail: jalujanm@cinvestav.mx*
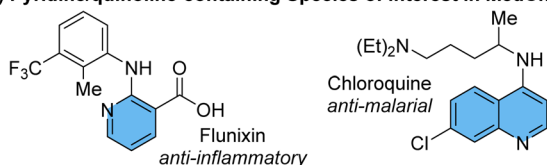
[b] *Departamento de Química, División de Ciencias Naturales y Exactas, Sede Noria Alta, Universidad de Guanajuato, Noria Alta s/n, C.P. 36050, Guanajuato, Gto., Mexico*

† Electronic supplementary information (ESI) available: Cartesian coordinates of the calculated reaction mechanism. See DOI: https://doi.org/10.1039/d4nj00913d
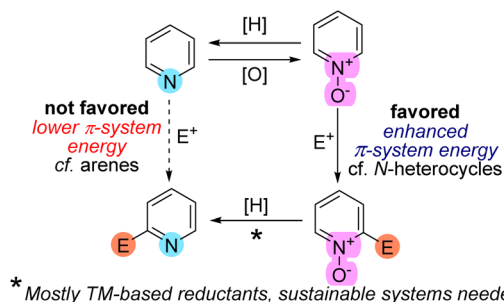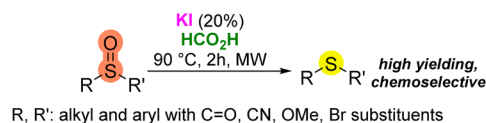
‡ Contributed equally.

a) Pyridine/quinoline-containing Species of Interest in MedChem

Flunixin
anti-inflammatory

Chloroquine
anti-malarial

b) Enhancing reactivity through pyridine/pyridine oxide interplay

not favored
lower π-system energy
cf. arenes

favored
enhanced π-system energy
cf. *N*-heterocycles

* *Mostly TM-based reductants, sustainable systems needed*

c) Previous work: I⁻/FA reagent for S=O desoxygenation

KI (20%)
HCO$_2$H
90 °C, 2h, MW

high yielding, chemoselective

R, R': alkyl and aryl with C=O, CN, OMe, Br substituents

d) This work

MgI$_2$ (10 mol%)
HCO$_2$H
MW, 140 °C

- **Iodide catalysis** - **Formic acid as a green sacrificial reductant** - **Highly selective**

Fig. 1 (a) Examples of relevant *N*-oxide pyridine species in medicinal chemistry (MedChem). (b) Pyridine *N*-oxide features enhanced reactivity compared to pyridine. (c) I⁻/FA reagent for the efficient reduction of sulfoxides (shown) and methyl sulfinates (not shown). (d) MgI$_2$ as a convenient iodide source for a TM-free reduction based on the I⁻/FA reagent.

Table 1 Halide source screening for the deoxygenation of quinoline 1-oxide (**1a**)

[I⁻] (x mol%)
HCO$_2$H
MW, 3 h 140 °C

Entry	Halide source [I⁻]	(% mol)	Time (h)	Yield (%)[a]
1	KI	10	1	40
2	—	—	1	—
3	K$_2$SO$_4$	10	1	—
4	K$_2$HPO$_4$	10	1	—
5	TBAI	10	1	39
6	NaI	10	1	37
7	KIO$_3$	10	1	37
8	ZnI$_2$	5	1	14
9	I$_2$	5	1	42
10	MgI$_2$	5	1	46
11	MgSO$_4$	5	1	—
12	MgI$_2$	5	3	57
13	MgI$_2$	10	1	47
14	**MgI$_2$**	**10**	**3**	**91/91**[b]
15	MgI$_2$	10	4	95/85[b]
16	MgCl$_2$	10	3	2
17	MgBr$_2$	10	3	2
18[c]	MgI$_2$	10	3	65/49[b]

[a] Determined by ¹H-NMR. [b] Isolated yields. [c] Reaction performed using a conventional heating reactor at 140 °C (Anton-Paar Monowave® 50).

Interestingly, sterically hindered 2,6-methylated pyridine *N*-oxides (**1e**, **1f**) underwent deoxygenation without any detrimental effects, yielding the corresponding pyridines with excellent yields. Furthermore, complete orthogonality was observed for carbonyl-containing *N*-oxides, such as 4-acetylpyridine *N*-oxide (**1h**) and 4-benzoylpyridine *N*-oxide (**1i**). These results significantly support a wider range of conditions under which the I⁻/FA reductive reagent is effective (90–140 °C), without affecting carbonyl groups.[21] Additionally, a cyano-substituted substrate (**1j**) and 6-MeO-quinoline *N*-oxide (**1m**) underwent chemoselective *N*-deoxygenation, producing the corresponding heterocycles with excellent yields.

Under standard conditions, 3-nitroquinoline *N*-oxide (**1k**) underwent reduction of both the *N*-oxide and nitro groups, accompanied by formylation to yield product **2ka**. In contrast, 2-aminopyridine *N*-oxide (**1g**) was deoxygenated with excellent yield and without formylation, a result attributed to the significant electronic differences between positions 2 and 3 on the pyridine ring.[22] After adjusting the reaction conditions, **2k** was successfully obtained with the nitro group remaining unaffected (see ESI†). As for 4-nitroquinoline *N*-oxide (**1l**), a Nef-type hydrolytic removal of the nitro group was impossible to avoid, delivering quinolin-4-(*H*)-one (**2l**) as the sole product.[23] All attempts to adjust the conditions to obtain the nitro-containing deoxygenated product were unsuccessful (see ESI†). Finally, *N*-oxides of tertiary amines such as **1n** and **1o** were obtained with particularly good yields. Importantly, in all successful experimental trials, the reactor vial was pressurized during the reaction process and maintained a high pressure (>10 psi) after cooling to room temperature, which is consistent with the release of CO$_2$ as byproduct.[24] Upon completion of the reductions, the reaction mixtures typically

TBAI, NaI, KIO$_3$, ZnI$_2$, I$_2$, and MgI$_2$ were also evaluated, with the last two (entries 9 and 10) exhibiting superior performance compared to KI. Although KI, I$_2$ and MgI$_2$ delivered comparable results in terms of yield, MgI$_2$ delivered better reproducibility and chemoselectivity, prompting us to proceed with it for subsequent experiments. We had prior evidence indicating that iodide demonstrated superior performance compared to other halides in similar reductions.[16] This was reinforced for the N–O reduction through additional experiments employing magnesium chloride and bromide (entries 16 and 17), delivering low conversion. No contribution from Mg²⁺ was observed, further supporting the role of iodide as the reducing entity in MgI$_2$ (*cf.* entries 10 and 11). From tuning of reaction conditions, we identified 10% mol of MgI$_2$ and 3 h of reaction time as optimal (entry 14). An additional experiment conducted with conventional heating underscored the necessity of microwave activation (*cf.* entries 13 and 18).[19,20]

With the optimal conditions at hand, diverse *N*-oxides with varying substituents were submitted to the optimal deoxygenation conditions. Isoquinoline, benzo[*h*]quinoline, and phenazine *N*-oxides (**1b–1d**) were successfully deoxygenated with comparable yields to those obtained using TM-based technologies (Table 2).[9]

Table 2 Substrate scope for the reduction of N-oxides

2a, 91%   2b, 73%   2c, 78%   2d, 90%

2e, 95%[a]   2f, 92%[b]   2g, 97%   2h, 93%

2i, 92%   2j, 87%   2k, 47%[c]   2ka, 55%

2l, 27%[d]   2m, 90%[a]   2n, 80%   2o, 86%

[a] Reaction time 5 h. [b] Reaction time 6 h. [c] Reaction time 10 h @ 100 °C.
[d] Determined by ^{1}H-NMR.

developed a brownish hue, indicative of the presence of molecular iodine.

To get insight in the reaction mechanism for the N–O reduction, we performed DFT calculations (see ESI,† for further details) employing pyridine N-oxide as a model and considering the optimal conditions above discussed. First, we explored the interaction between MgI$_2$ and solvent molecules (Fig. 2). In a recent previous work, we demonstrated that the coordination modes of the Mg metal center vary based on the σ-donor capability of the Lewis base.[25] Consequently, FA acts as a ligand and magnesium can coordinate up to four units, through the carbonyl O atom, resulting in Mg–O–C angles of approximately 120°. Contrary to what one might expect, FA-ligands are monodentate and not bidentate. The formation of the lower coordination modes **A-1** and **A-2** is spontaneous, while the penta- and hexa-coordinated species, **A-3** and **A-4**, corresponding to sp^{3}d and sp^{3}d^2 hybridizations at the Mg center, exist in equilibrium with the tetrahedral **A-2** mode. The NOD mechanistic pathway and the subsequent iodide regeneration begins with a double substitution of iodide for two FA-ligands within the Mg coordination sphere (**A-4** → **I-1** → **I-2**, Fig. 3). The formation of the [Mg^{2+}(OCHOH)$_6$]2I$^-$ complex (**I-2**) requires $\Delta G_{A-4 \to I-2} = +4.2$ kcal mol^{-1}. Subsequently, the spontaneous addition of a pyridine N-oxide (C$_5$H$_5$NO) unit forms **I-3** ($\Delta G_{I-2 \to I-3} = -4.5$ kcal mol^{-1}). This addition is deemed favorable due to the hydrogen bonding between the oxygen in pyridine N-oxide and protons from formic acid units. Despite the
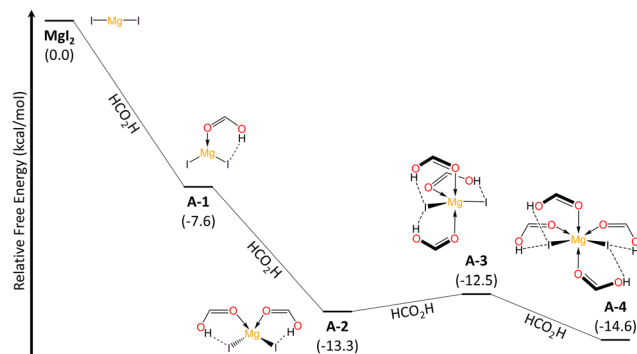

Fig. 2 Relative Gibbs free energy (kcal mol^{-1}) profile for the progressive coordination of formic acid ligands to MgI$_2$ at the (SMD:HCO$_2$H)ωB97X-D/def2-TZVPP//ωB97X-D/def2-SVP level and 298.15 K.

pKa values of pyridine N-oxide (0.79)[26] and formic acid (3.5)[27] suggesting that proton transfer (PT) between these Brønsted species might not be favored, our findings show that this process is both barrierless and exergonic ($\Delta G_{I-3 \to I-4} = -3.5$ kcal mol^{-1}). Thus, it seems that an effect of increased acidity of FA protons, through Mg-FA coordination, facilitates the PT process to access **I-4** effortlessly. Next, a nucleophilic substitution (S$_N$2-type) takes place, centered on the oxygen atom via **TS-1** ($\Delta G^{\ddagger}_{I-4 \to TS-1} = +32.5$ kcal mol^{-1}, in agreement with $T = 140$ °C), marking the rate-determining step and resulting in the formation of the pyridine-hypoiodous acid pair in **I-5**. Remarkably, formic acid acts as a Brønsted-activator enabling the electrophilicity of the pyridine N-oxide, so the nucleophilic attack of iodide is feasible. From **I-5**, a hydrogen transfer process was determined via **TS-2A**, with an energy barrier of $\Delta G^{\ddagger}_{I-5 \to TS-2A} = +20.1$ kcal mol^{-1}, leading to the production of hydroiodic acid and carbon dioxide (**P-A**) through a net exothermic process. Then, hydroiodic acid spontaneously transfers its proton to the pyridine supported by a H$_2$O unit.

We identified an equilibrium between **I-5** and a formyl hypoiodite species (**I-6**, $\Delta G_{I-5 \to I-6} = -1.9$ kcal mol^{-1}). Finding a transition state connecting these minima proved to be difficult. Starting from **I-6**, **I-5** can also lead to the formation of molecular iodine (I$_2$, **P-B**) through iodide addition, with an energy barrier of $\Delta G^{\ddagger}_{I-6 \to TS-2B} = +9.6$ kcal mol^{-1}. These equilibria towards non-iodide productive species determines the molar percentage required for the iodide reactant, as amounts of MgI$_2$ lower than standard significantly affect the conversion rate (cf. entries 12,14, Table 1). However, our thermochemical data suggest that iodine (**P-B**) can be converted into **P-A** by accessing **I-5** and then proceeding through **TS-2A**, requiring an energy investment of $\Delta G^{\ddagger}_{P-B \to TS-2A} = +33.1$ kcal mol^{-1}.

Conclusions

We developed a methodology with a sustainable basis for the deoxygenation of pyridine N-oxides, as formic acid is employed as activator, solvent, and stoichiometric reductant, using MgI$_2$ as a convenient iodide source, which serves as a catalytic reductant. This method proved to be compatible with various potentially reducible functional groups, including carbonyl, cyano, benzyl, and to some extent, the nitro group. The same
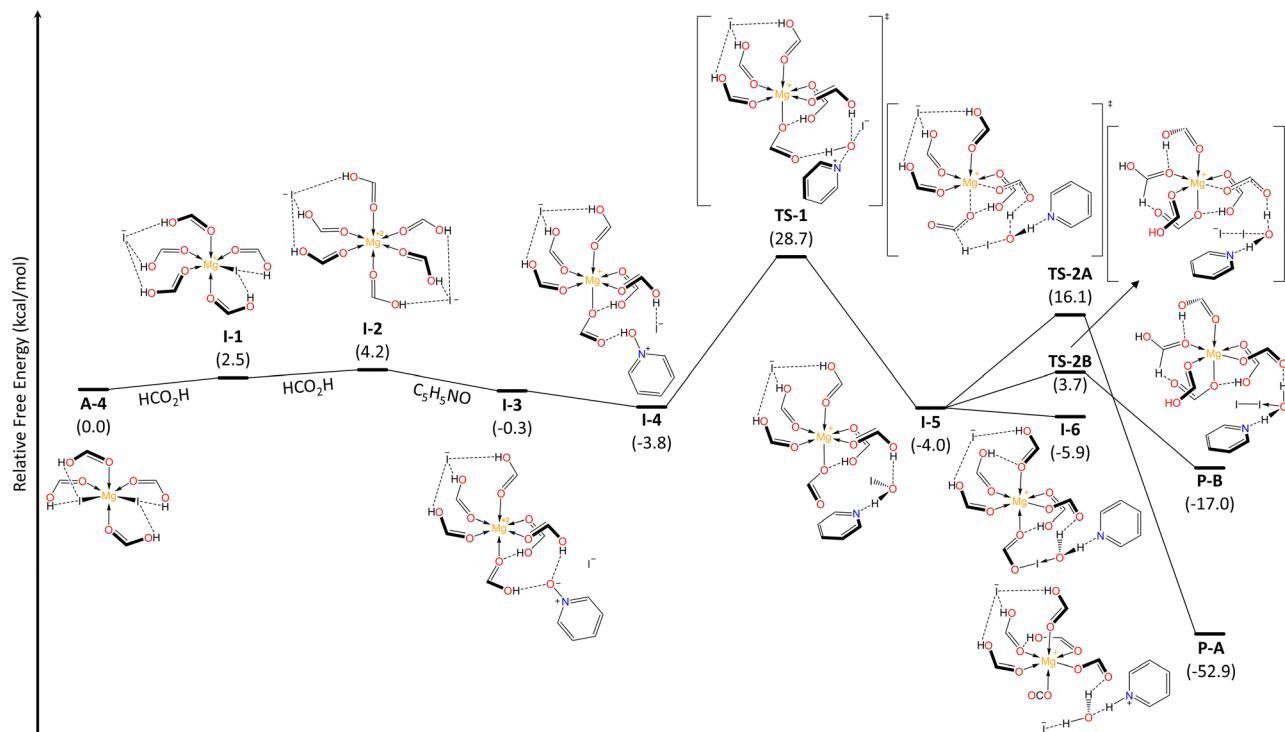
Fig. 3 Relative Gibbs free energy (kcal mol^{-1}) profile for the pyridine *N*-oxide deoxygenation using FA-coordinated MgI$_2$ (**A-4**) at the (SMD:HCO$_2$-H)ωB97X-D/def2-TZVPP//ωB97X-D/def2-SVP level and 298.15 K.

system also allowed for the deoxygenation of tertiary amines. The mechanistic study through DFT suggests that the *N*-oxide deoxygenation occurs *via* an S$_N$2-type mechanism. Formic acid performs Brønsted-activation, increasing its acidity through Mg^{2+} coordination (Lewis to Brønsted acid relay). Also, the molar concentration of MgI$_2$ must be such to overcome non-iodide productive oxidized iodine species, such as I$_2$. The regeneration of iodide mainly occurs through the reduction of hypoiodous acid by hydrogen transfer delivering a net exothermic process. To regenerate iodide from molecular iodine, the pathway involves the reversion towards hypoiodite followed by hydrogen transfer, requiring +33.1 kcal mol^{-1} to complete the reduction.

Conflicts of interest

There are no conflicts to declare.

Acknowledgements

Notes and references

1 M. F. Grundon, *Nat. Prod. Rep.*, 1984, **1**, 195–200.
2 Selected literature: (*a*) T. Tahir, M. Ashfaq, M. Saleem, M. Rafiq, M. I. Shahzad, K. Kotwica-Mojzych and M. Mojzych, *Molecules*, 2021, **26**, 4872; (*b*) B. S. Matada, R. Pattanashettar and N. G. Yernale, *Bioorg. Med. Chem.*, 2021, **32**, 115973; (*c*) H. William, K. Kutterer, A. Crombie and J. Clemens, *Prog. Heterocycl. Chem.*, 2009, **6**, 289–332; (*d*) A. Y. Khan and G. Suresh Kumar, *Biophys. Rev.*, 2015, **7**, 407–420.
3 Selected literature: (*a*) R. Kaur and K. Kumar, *Eur. J. Med. Chem.*, 2021, **215**, 113220; (*b*) P. E. Alford. Six-Membered Ring Systems: Pyridines and Benzo Derivatives. in *Progress in Heterocyclic Chemistry*, vol. 22, ed. G. Gribble and J. A. Joule, Elsevier, 2011, pp. 349–391; (*c*) E. Vitaku, D. T. Smith and J. T. Njardarson, *J. Med. Chem.*, 2014, **57**, 10257–10274; (*d*) A. Basnet, P. Thapa, R. Karki, Y. Na, Y. Jahng, B. S. Jeong, T. C. Jeong, C. S. Lee and E. S. Lee, *Bioorg. Med. Chem.*, 2007, **15**, 4351–4359; (*e*) G. Bentzinger, E. Pair, J. Guillon, M. Marchivie, C. Mullié, P. Agnamey, A. Dassonville-Klimpt and P. Sonnet, *Tetrahedron*, 2020, **76**, 131088.
4 Selected literature: (*a*) S. Varshney and N. Mishra. Pyridine-based polymers and derivatives: Synthesis and applications.

in *Recent Developments in the Synthesis and Applications of Pyridines*, ed P. E. Singh, Elsevier, 2022, pp. 43–69; (b) K. Kumar, A. Karmakar, F.-R. Chen, J.-H. Jou, S. Ghosh, S. Banik and S. Kumar, *Phys. Chem. Chem. Phys.*, 2023, **25**, 19648–19659; (c) C. Verma, K. Y. Rhee, M. A. Quraishi and E. E. Ebenso, *J. Taiwan Inst. Chem. Eng.*, 2020, **117**, 265–277.

5 (a) J. S. Carey, D. Laffan, C. Thomson and M. T. Williams, *Org. Biomol. Chem.*, 2006, **4**, 2337–2347; (b) S. De, A. Kumar, S. K. Shah, S. Kazi, N. Sarkar, S. Banerjee and S. Dey, *RSC Adv.*, 2022, **12**, 15385–15406.

6 A. Katritzky and R. Taylor *Heteroaromatics Containing One Six-Membered Ring. In Advances in Heterocyclic Chemistry*, Academic Press, 1990, vol. 47, pp. 277–323.

7 J. A. Bull, J. J. Mousseau, G. Pelletier and A. B. Charrette, *Chem. Rev.*, 2012, **112**, 2642–2713.

8 (a) D. Wang, L. Désaubry, G. Li, M. Huang and S. Zheng, *Adv. Synth. Catal.*, 2021, **363**, 2–39; (b) R. Tomar, A. Kumar, A. Dalal, D. Bhattacharya, P. Singh and S. Arulananda Babu, *Asian J. Org. Chem.*, 2022, **11**, e202200311; (c) J. Zhong, Y. Long, X. Yan, S. He, R. Ye, H. Xiang and X. Zhou, *Org. Lett.*, 2019, **21**, 9790–9794; For a recent *umpolung* strategy for the electrophilic functionalization of *N*-oxides see: (d) D. I. Bugaenko, M. A. Yurovskaya and A. V. Karchava, *Org. Lett.*, 2021, **23**, 6099–6104.

9 Selected literature: (a) J. Li, S. Liu, T. L. Lohr and T. J. Marks, *ChemCatChem*, 2019, **11**, 4139–4146; (b) R. Rubio-Presa, M. A. Fernández-Rodríguez, M. R. Pedrosa, F. J. Arnáiz and R. Sanz, *Adv. Synth. Catal.*, 2017, **359**, 1752–1757; (c) Y. Kuwahara, Y. Yoshimura, K. Haematsu and H. Yamashita, *J. Am. Chem. Soc.*, 2018, **140**, 9203–9210; (d) K. D. Kim and J. Lee, *Org. Lett.*, 2018, **20**, 7712–7716; (e) Y. Handa, J. Inanaga and M. Yamaguchi, *J. Chem. Soc., Chem. Commun.*, 1989, 298–299; (f) J. A. Fuentes and M. L. Clarke, *Synlett*, 2008, 2579–2582; (g) B. W. Yoo and J. W. Choi, *Synth. Commun.*, 2009, **39**, 3550–3554.

10 Selected literature: (a) Y. Kawazoe and M. Tachibana, *Chem. Pharm. Bull.*, 1965, **13**, 1103–1107; (b) S. R. Ram, K. P. Chary and D. S. Iyengar, *Synth. Commun.*, 2000, **30**, 3511–3515; (c) H. P. Kokatla, P. F. Thomson, S. Bae, V. R. Doddi and M. K. Lakshman, *J. Org. Chem.*, 2011, **76**, 7842–7848; (d) H. Suzuki, N. Sato and A. Osuna, *Chem. Lett.*, 1980, **9**, 459–460; (e) A. Romero and H. Cerecetto, *Eur. J. Org. Chem.*, 2020, 1853–1865.

11 D. S. Raghuvanshi, N. Verma and A. Gupta, *ChemistrySelect*, 2019, **4**, 2075–2078.

12 T. B. Nguyen, L. Ermolenko and A. Al-Mourabit, *Green Chem.*, 2016, **18**, 2966–2970.

13 Selected literature: (a) T. Morita, K. Kuroda, Y. Okamoto and H. Sakurai, *Chem. Lett.*, 1981, **10**, 921–924; (b) R. Balicki, *Chem. Ber.*, 1990, **123**, 647–648; (c) B. W. Yoo and M. C. Park, *Synth. Commun.*, 2008, **38**, 1646–1650; (d) B. W. Yoo, J. W. Choi and S. Park, *Bull. Korean Chem. Soc.*, 2008, **29**, 909–910; (e) M. M. Khodaei, A. Alizadeh and H. A. Hezarkhani, *J. Iran. Chem. Soc.*, 2018, **15**, 1843–1849; (f) M. Boruah and D. Konwar, *Synlett*, 2001, 795–796.

14 Selected literature: (a) D. Wang and D. Astruc, *Chem. Rev.*, 2015, **115**, 6621–6686; (b) D. Formenti, F. Ferretti, F. K. Scharnagl and M. Beller, *Chem. Rev.*, 2019, **119**, 2611–2680; (c) L.-H. Gong,

Y.-Y. Cai, X.-H. Li, X. Y.-N. Zhang, J. Su and J.-S. Chen, *J. Green Chem.*, 2014, **16**, 3746–3751.

15 (a) D. J. Hayes, S. Fitzpatrick, M. H. B. Hayes and J. R. H. Ross. The Biofine Process – Production of Levulinic Acid, Furfural, and Formic Acid from Lignocellulosic Feedstocks. in *Biorefineries-Industrial Processes and Products: Status Quo and Future Directions*. ed. B. Kamm, P. R. Gruber and M. Kamm, Wiley, 2005, pp. 139–164; (b) K. Sordakis, C. Tang, L. K. Vogt, H. Junge, P. J. Dyson, M. Beller and G. Laurenczy, *Chem. Rev.*, 2018, **118**, 372–433.

16 J. A. Luján-Montelongo, L. J. García de la Cuesta, A. E. Cruz-Jiménez, P. Hernández and A. Vela, *Green Chem.*, 2023, **25**, 7963–7970.

17 O. A. Valle-González, Á. I. Salazar-Bello and J. A. Luján-Montelongo, *Org. Biomol. Chem.*, 2023, **21**, 2894–2898.

18 J. A. Luján-Montelongo, J. B. Mateus-Ruiz and R. M. Valdez-García, *Eur. J. Org. Chem.*, 2023, **26**, e202201156.

19 (a) G. B. Dudley, R. Richert and A. E. Stiegman, *Chem. Sci.*, 2015, **6**, 2144–2152; (b) J. Zhou, W. Xu, Z. You, Z. Wang, Y. Luo, L. Gao, C. Yin, R. Peng and L. Lan, *Sci. Rep.*, 2016, **6**, 25149.

20 A Biotage® Initiator+ microwave reactor and 0.5-2 mL reaction tubes were used in the N-O deoxygenation reactions. The radiation absorption parameter was set to VERY HIGH, with the apparatus usually recording a pressure increase (10-20 Psi).

21 The sulfinyl reduction with I⁻/FA usually is carried out at 90 °C (see reference 16) whereas heterocyclic N-oxides required 140 °C. For selected literature featuring C-O bond reductions involving iodide: (a) L. D. Hicks, J. K. Han and A. J. Fry, *Tetrahedron Lett.*, 2000, **41**, 7817–7820; (b) M. Allukian, G. Han, L. Hicks and A. J. Fry, *ARKIVOC*, 2002, 76–79; (c) J. E. Milne, T. Storz, J. T. Colyer, O. R. Thiel, M. D. Seran, R. D. Larsen and J. A. Murry, *J. Org. Chem.*, 2011, **76**, 9519–9524; (d) L.-Z. Yuan, D. Renko, I. Khelifi, O. Provot, J.-D. Brion, A. Hamze and M. Alami, *Org. Lett.*, 2016, **18**, 3238–3241; (e) L.-Z. Yuan, G. Zhao, A. Hamze, M. Alami and O. Provot, *Adv. Synth. Catal.*, 2017, **359**, 2682–2691.

22 Recently, a formylation of primary and secondary amines under comparable conditions was demonstrated: H. Liang, T. Zhao, J. Ou, J. Liu and X. Hu, *ACS Sustainable Chem. Eng.*, 2023, **11**, 14317–14322.

23 J. Xu, X. Miao, L. Liu, Y. Wang and W. Yang, *ChemSusChem*, 2021, **14**, 5311–5319.

24 N. D. Rode, A. Arcadi, M. Chiarini and F. Marinelli, *Synthesis*, 2017, **49**, 2501–2512.

25 L. I. Lugo-Fuentes, V. A. Lucas-Rosales, J. A. Sandoval-Mendoza, R. Shang, J. P. Martínez and J. O. C. Jimenez-Halla, *Chem. – Eur. J.*, 2024, **30**, e202304130.

26 (a) L. Chmurzyński, *Anal. Chim. Acta*, 1996, **321**, 237–244; (b) P. Mech, M. Bogunia, A. Nowacki and M. Makowski, *J. Phys. Chem. A*, 2020, **124**, 538–551.

27 (a) M. H. Kim, C. S. Kim, H. W. Lee and K. Kim, *J. Chem. Soc., Faraday Trans.*, 1996, **92**, 4951–4956; (b) X.-x. Wang, H. Fu, D.-m. Du, Z.-y. Zhou, A.-g. Zhang, C.-f. Su and K.-s. Ma, *Chem. Phys. Lett.*, 2008, **460**, 339–342; (c) F. R. Dutra, C. de S. Silva and R. Custodio, *J. Phys. Chem. A*, 2021, **125**, 65–73.